nature photonics

LETTERS

https://doi.org/10.1038/s41566-018-0320-3

Coherent injection locking of quantum cascade laser frequency combs

Johannes Hillbrand[1], Aaron Maxwell Andrews[1,2], Hermann Detz[1,3], Gottfried Strasser[1,2] and Benedikt Schwarz[1*]

Quantum cascade laser (QCL) frequency combs are a promising candidate for chemical sensing and biomedical diagnostics[1–4]. They are electrically pumped and compact, making them an ideal platform for on-chip integration[5]. Until now, optical feedback is fatal for frequency comb generation in QCLs[6]. This property limits the potential for integration. Here, we demonstrate coherent electrical injection locking of the repetition frequency to a stabilized radio-frequency oscillator. We prove that the injection-locked QCL spectrum can be phase-locked, resulting in the generation of a frequency comb. We show that injection locking is not only a versatile tool for all-electrical frequency stabilization, but also mitigates the fatal effect of optical feedback. A prototype self-detected dual-comb set-up consisting only of an injection-locked dual-comb chip, a lens and a mirror demonstrates the enormous potential for on-chip dual-comb spectroscopy. These results pave the way to miniaturized and all-solid-state mid-infrared spectrometers.

Optical frequency combs are lasers whose spectrum consists of a multitude of equidistant lines[7]. They have emerged as high-precision tools for time metrology, frequency synthesis and spectroscopy[8–10]. The mid-infrared region is of particular interest for spectroscopic applications because most molecules exhibit fundamental rotovibrational absorption lines in this portion of the electromagnetic spectrum[11,12]. In the past decade, the quantum cascade laser[1] (QCL) has become the dominant source of coherent mid-infrared light. Thanks to the large third-order optical nonlinearity of their active regions, the longitudinal cavity modes of Fabry–Pérot QCLs can be locked to each other by four-wave-mixing, resulting in the generation of phase-coherent frequency combs[2,13]. The equidistant teeth of the comb beat together, causing a modulation of the laser intensity at the cavity roundtrip frequency. In the comb regime, all cavity modes are equidistant, which results in a narrow and stable beatnote with linewidths on the hertz-level. Depending on the laser bias, a second regime called the high phase-noise regime is observed, where increased amplitude and phase-noise of the comb lines result in a considerably broader beatnote. This regime is caused by the finite laser dispersion[14] and limits the applicability of the combs for dual-comb spectroscopy[4]. Due to the fast carrier dynamics in QCL active regions, the beating of the comb lines induces a temporal modulation of the population inversion. This population pulsation results in a macroscopic current modulation, enabling the direct observation of the so-called electrical beatnote.

As a general property of any oscillator, its frequency and phase can be locked to another oscillator provided that there is enough coupling[15]. Consequently, an external radio-frequency (RF) modulation close to the roundtrip frequency injected into the QCL should be able to influence or even lock the electrical beatnote. This concept is called electrical injection locking and was demonstrated in terahertz QCLs[16,17] and later in mid-infrared QCLs by embedding a Fabry–Pérot cavity into a microstrip RF waveguide[18]. Although this result proves that the collective action of the beatings of adjacent comb lines can be locked, it remains unclear to what extent the single beatings are locked and what their phases are. Indeed, another experiment revealed that the narrow beatnote of an injection-locked QCL was produced by only a few modes, whereas the rest of the spectrum remained unlocked[2].

In this Letter, we provide conclusive proof that all teeth of the comb can be locked coherently to an external RF source by applying the RF signal only to the end of the laser cavity. In this section of the cavity, the electrical beating is most susceptible to the injected signal due to its inherent spatiotemporal pattern that was revealed by recent work[19]. A schematic is shown in Fig. 1.

Proving frequency comb operation of a QCL is a challenging task because the fast gain recovery time prevents the formation of short and intense pulses. Consequently, traditional methods based on nonlinear autocorrelation techniques[20,21] cannot be employed. Instead, we use a linear phase-sensitive autocorrelation method called 'Shifted Wave Interference Fourier Transform Spectroscopy'[22,23] (SWIFTS, Fig. 2a). SWIFTS enables the direct measurement of the phase coherence of the emitted comb spectrum (details in Methods). Moreover, the complex phase of the SWIFTS spectrum is equal to the phase difference of adjacent comb lines. In more detail, one can define a normalized intermodal coherence[23]:

$$c = \frac{|\langle A_n A_{n-1} e^{(i(\phi_n - \phi_{n-1}))}\rangle|}{\langle |A_n|\,|A_{n-1}|\rangle} \quad (1)$$

Here, A_n are the electric field amplitudes of the comb modes, ϕ_n are the corresponding phases and the angled brackets denote temporal averaging. If two modes are fully coherent (that is, phase-locked), the SWIFTS amplitude is commensurate with the geometric average of the amplitudes of the intensity spectrum $|A_n||A_{n-1}|$ and c is unity. If, however, the relative phase noise of a mode pair is non-zero, the SWIFTS amplitude decreases due to the temporal averaging and c drops below unity.

Figure 2b shows the intensity and SWIFTS interferograms of the free-running QCL comb (that is, without RF injection). Interestingly, both SWIFTS quadratures have a minimum at zero path difference of the FTIR mirrors, whereas the intensity interferogram has its maximum there. This phenomenon is related to the

[1]Institute of Solid State Electronics, TU Wien, Vienna, Austria. [2]Center for Micro- and Nanostructures, TU Wien, Vienna, Austria. [3]CEITEC, Brno University of Technology, Brno, Czech Republic. *e-mail: benedikt.schwarz@tuwien.ac.at

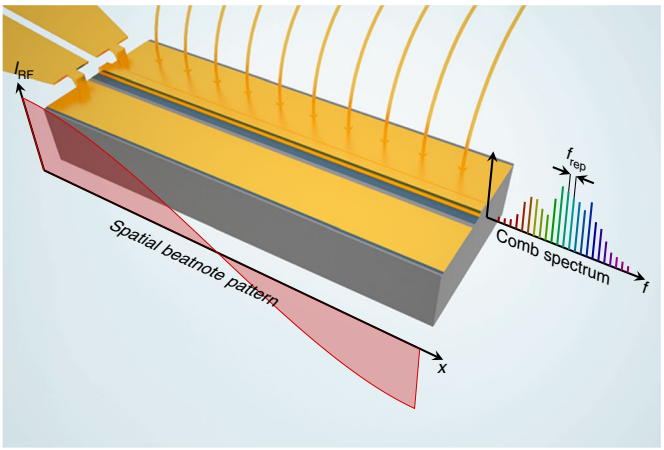

Fig. 1 | Schematic of the device. Injection locking of the coherent beating in a QCL frequency comb using a RF probe touched down on top of the edge of the laser cavity. The spatial pattern of the electrical beatnote is highlighted in red. Due to the standing waves in the Fabry–Pérot cavity, the amplitude of the beatnote follows $I \propto \cos(\pi x/L)\cos(2\pi f_{rep} t)$, where L is the cavity length and f_{rep} the repetition frequency.

fast gain dynamics of QCL active regions, which favour comb states with minimal amplitude modulation of the laser intensity[2,24,25]. The SWIFTS spectrum (Fig. 2c) has the same shape as the intensity spectrum, without showing any spectral holes. This proves that indeed all teeth of the comb are phase-locked. The SWIFTS phases—that is, the phase difference of adjacent comb lines—cover a range of 2π from the lowest to the highest frequency mode. This corresponds to a strongly frequency modulated output of the QCL with a linearly chirped instantaneous frequency[26]. We attribute the origin of this characteristic phase pattern to the fast gain dynamics of the QCL, which are fast enough to follow several harmonics of the cavity roundtrip frequency. As a consequence, the population inversion oscillates in anti-phase with respect to the beating of the intracavity field, thus leading to a phase-sensitive loss mechanism called parametric suppression[25]. Hence, the QCL favours states with minimal amplitude modulation so as to mitigate population pulsations and parametric suppression. It can be shown analytically that a difference phase pattern, which increases linearly between 0 and 2π, minimizes the beating at all harmonics of f_{rep} for a uniform comb spectrum (Supplementary Fig. 2). This is in accordance with the observed minimum of the SWIFTS interferograms at zero path difference (Fig. 2b).

The first challenge to prove coherent injection locking is to show the capability to lock the QCL beatnote to the external oscillator. To do so, we drive the QCL at a bias where it operates in the high phase-noise regime (Supplementary Fig. 3) and shine it directly on the fast QWIP. We then record the RF spectrum of the QWIP current with a spectrum analyser (Fig. 3a). As the injected RF power is increased, the broad beatnote is pulled towards the frequency of the injected signal, and finally locks at 8 dBm. Two side peaks that are roughly 20 dB weaker than the initial beatnote remain. At 12 dBm, also these side peaks vanish and the microwave spectrum of the optical beating is fully controlled by the injected signal. The noise floor around the locked narrow beatnote is roughly 30 dB weaker than the peak power of the originally broad beatnote. This proves that the vast majority of the optical beatnote power is locked. To highlight spectral regions which are locked to the external oscillator, we measure the intermodal coherence and the intensity spectrum as functions of the injected power (Fig. 3b, c). The intermodal coherence starts to grow considerably at 5 dBm—equal to the power level at which the broad beatnote in Fig. 3a is pulled towards the injection frequency. Finally, the entire emission spectrum is locked at 12 dBm. A detailed snapshot of the SWIFTS characterization at 12 dBm RF power (Fig. 3d) shows that the SWIFTS amplitudes are commensurate with the values expected from the intensity spectrum. This proves that the entire spectrum of the QCL is phase locked to the RF oscillator. The SWIFTS phases feature the same phase pattern as observed in free-running comb operation (Fig. 2c). It is remarkable that the frequencies of the intermode beatings are locked to the external modulation although their phases do not synchronize in phase with the injected signal. This suggests that the injected signal is strong enough to synchronize the intermode difference frequencies, but too weak to overcome the effect of parametric suppression. A more detailed description of the underlying coupling

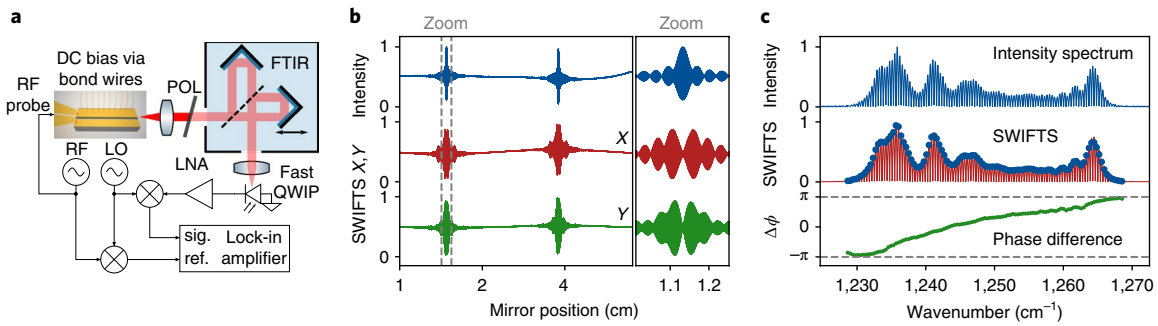

Fig. 2 | SWIFTS analysis of the free-running comb. a, SWIFTS set-up. The light emitted by the QCL is shone through a Fourier transform infrared (FTIR) spectrometer. The optical beatnote of the QCL is detected by a fast quantum well infrared photodetector (QWIP)[29], amplified by a low-noise amplifier (LNA) and mixed down to approximately 40 MHz using a local oscillator (LO). The mixing product of the LO and the oscillator used for injection locking (RF) acts as reference for a lock-in amplifier. By measuring the two quadratures X and Y of the optical beatnote as functions of the mirror delay τ, the complex interferogram of the portion of light that is locked to the RF oscillator is obtained. Subsequently, the SWIFTS spectrum is retrieved by applying a fast Fourier transform to the complex interferogram. A polarizer (POL) is used for adjustable attenuation. **b**, Intensity and SWIFTS quadrature interferograms of the free-running QCL frequency comb with a zoomed view around zero path. Here, the electrical beatnote of the QCL is used as phase reference for the lock-in amplifier. **c**, Intensity spectrum (blue line), SWIFTS spectrum (red line) with expected SWIFTS amplitudes for full coherence (blue dots), as well as the phase differences between adjacent comb lines retrieved from the SWIFTS data (green dots). The corresponding reconstructed time domain signal can be found in Supplementary Fig. 1.

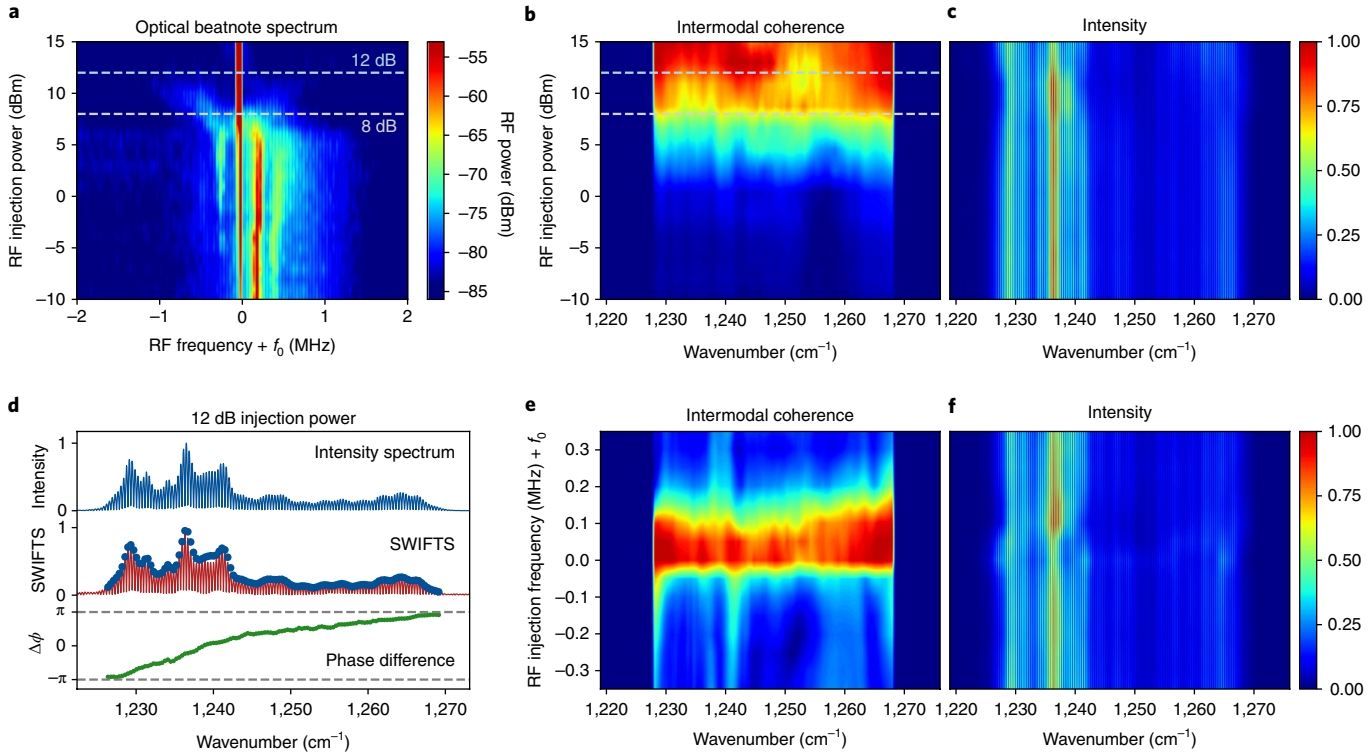

Fig. 3 | Coherent injection locking. a, Radio-frequency spectra of the optical beatnote around $f_0 \approx 11$ GHz, depending on the RF injection power recorded with the QWIP. The injection frequency is held constant at approximately 100 kHz below the beatnote frequency. The two sidebands above and below the frequency of the optical beatnote are caused by the mixing of the beatnote and the injected signal. **b**, Normalized intermodal coherence as a function of the injected power. The small spectral hole around 1,252 cm^{-1} is caused by the small laser intensity. **c**, Corresponding intensity spectrum. **d**, Detailed SWIFTS characterization at 12 dBm. **e**, Normalized intermodal coherence for different injection frequencies at 12 dBm injected power. **f**, Corresponding intensity spectrum. The corresponding optical beatnote spectrum is shown in Supplementary Fig. 4. The detailed SWIFTS characterization of the partially coherent state is shown in Supplementary Fig. 5.

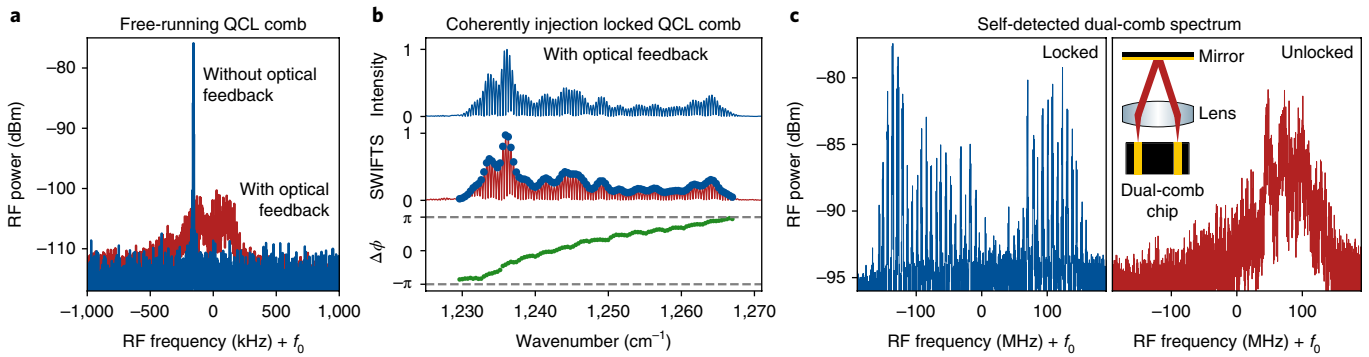

Fig. 4 | Comb operation under strong optical feedback. a, Electrical beatnote of the free-running QCL around $f_0 \approx 11$ GHz without (blue line) and with (red line) strong optical feedback. Sweep time = 2.4 s. **b**, SWIFTS characterization of the injection-locked QCL in the presence of intense optical feedback. The periodic modulation of the optical spectrum and the phases is caused by Fabry–Pérot resonances and the Gires–Tournois effect in the Si wafer. The SWIFTS analysis in the same state without optical feedback is shown in Supplementary Fig. 7. **c**, Self-detected multiheterodyne beat spectrum at $f_0 = 8.7$ GHz of two QCLs that shine directly into each other (inset). The dual-comb spectrum (blue line) changes to a broad multiheterodyne beat (red line) when the injection frequency of one laser is detuned out of the locking range by 200 kHz. This experiment can also be carried out using an external fast QWIP (Supplementary Fig. 8).

mechanisms is given in Supplementary Fig. 6. To investigate the influence of the injection frequency on the coherence of the QCL, we sweep it across the broad beatnote. The colour plot of the normalized coherence (Fig. 3e,f) shows that the QCL is locked to the injected signal in a narrow range of approximately 100 kHz around the frequency of the beatnote. Outside this locking range, only a few modes show non-negligible coherence.

In real-life applications, QCL frequency combs have to withstand harsh conditions while maintaining coherence. Among these conditions is optical feedback. We illustrate the fatal effect of optical

feedback on a free-running QCL frequency comb by replacing the attenuating polarizer (POL in Fig. 2a) by a polished silicon wafer perpendicular to the QCL beam. In this configuration, the QCL is subject to both intense static feedback from the Si wafer as well as temporally varying feedback from the QWIP facet due to the scanning FTIR mirrors. Whereas the electrical beatnote is narrow and stable if the beam is attenuated by the polarizer (Fig. 4a), it becomes broader and weaker upon exposure to strong optical feedback, indicating the loss of coherence. This fatal effect of optical feedback is omnipresent in dual-comb spectrometers based on QCL combs. Expensive and bulky optical isolators have to be employed to ensure stable comb operation, impairing the capabilities of miniaturization. In contrast, both the coherence and the phase characteristics of an injection-locked comb are preserved even in the presence of strong optical feedback (Fig. 4b). A prototype self-detected dual-comb set-up highlights the enormous potential of coherent electrical injection locking for miniaturization. The light of two QCLs located on the same chip is shone directly into each other without any optically isolating elements between (Fig. 4c). When both lasers are locked, the self-detected dual-comb beat spectrum consists of numerous equidistant lines with a spacing of $\Delta f_{rep} = 7.4$ MHz. The linewidth of the dual-comb beatings can be further reduced by applying computational phase correction[27]. If the injection frequency of one laser is detuned by 200 kHz—thus leaving the locking range (Fig. 3e)—the multiheterodyne signal becomes broad and dual-comb lines are no longer visible. These results open up new avenues towards all-solid-state mid-infrared spectrometers[28], where the ability to cope with intense feedback is vital.

Our investigations demonstrate that electrical injection locking of mid-infrared QCLs is a versatile technique that enables the generation of coherent frequency combs if the inherent spatiotemporal pattern of the electrical beatnote is taken into account. The fact that the repetition frequency is fixed by the injected signal can be used to stabilize the carrier envelope offset frequency against a narrow molecular absorption line via the driving current (Supplementary Fig. 9). The possibility of all-electric stabilization using low-budget electronics, such as those found in every mobile phone, will lead to a new class of miniaturized dual-comb spectrometers.

Online content

Any methods, additional references, Nature Research reporting summaries, source data, statements of data availability and associated accession codes are available at https://doi.org/10.1038/s41566-018-0320-3.

Received: 3 July 2018; Accepted: 12 November 2018;
Published online: 10 December 2018

References

1. Faist, J. et al. Quantum cascade laser. *Science* **264**, 553–556 (1994).
2. Hugi, A., Villares, G., Blaser, S., Liu, H. C. & Faist, J. Mid-infrared frequency comb based on a quantum cascade laser. *Nature* **492**, 229–233 (2012).
3. Geiser, M. et al. Single-shot microsecond-resolved spectroscopy of the bacteriorhodopsin photocycle with quantum cascade laser frequency combs. *Biophys. J.* **114**, 173a (2018).
4. Villares, G., Hugi, A., Blaser, S. & Faist, J. Dual-comb spectroscopy based on quantum-cascade-laser frequency combs. *Nat. Commun.* **5**, 5192 (2014).
5. Villares, G. et al. On-chip dual-comb based on quantum cascade laser frequency combs. *Appl. Phys. Lett.* **107**, 251104 (2015).
6. Jouy, P. et al. Dual comb operation of $\lambda \sim 8.2$ μm quantum cascade laser frequency comb with 1 W optical power. *Appl. Phys. Lett.* **111**, 141102 (2017).
7. Udem, T., Holzwarth, R. & Hänsch, T. W. Optical frequency metrology. *Nature* **416**, 233–237 (2002).
8. Udem, T., Reichert, J., Holzwarth, R. & Hänsch, T. W. Absolute optical frequency measurement of the Cesium D_1 line with a mode-locked laser. *Phys. Rev. Lett.* **82**, 3568–3571 (1999).
9. Holzwarth, R. et al. Optical frequency synthesizer for precision spectroscopy. *Phys. Rev. Lett.* **85**, 2264–2267 (2000).
10. Bernhardt, B. et al. Cavity-enhanced dual-comb spectroscopy. *Nat. Photon.* **4**, 55–57 (2009).
11. Haas, J. & Mizaikoff, B. Advances in mid-infrared spectroscopy for chemical analysis. *Annu. Rev. Anal. Chem.* **9**, 45–68 (2016).
12. Waclawek, J. P. et al. Quartz-enhanced photoacoustic spectroscopy-based sensor system for sulfur dioxide detection using a CW DFB-QCL. *Appl. Phys. B* **117**, 113–120 (2014).
13. Friedli, P. et al. Four-wave mixing in a quantum cascade laser amplifier. *Appl. Phys. Lett.* **102**, 222104 (2013).
14. Faist, J. et al. Quantum cascade laser frequency combs. *Nanophotonics* **5**, 272–291 (2016).
15. Razavi, B. A study of injection locking and pulling in oscillators. *IEEE J. Solid-State Circuit* **39**, 1415–1424 (2004).
16. Gellie, P. et al. Injection-locking of terahertz quantum cascade lasers up to 35 GHz using RF amplitude modulation. *Opt. Express* **18**, 20799–20816 (2010).
17. Barbieri, S. et al. Coherent sampling of active mode-locked terahertz quantum cascade lasers and frequency synthesis. *Nat. Photon.* **5**, 306–313 (2011).
18. St-Jean, M. R. et al. Injection locking of mid-infrared quantum cascade laser at 14 GHz, by direct microwave modulation. *Laser Photon. Rev.* **8**, 443–449 (2014).
19. Piccardo, M. et al. Time-dependent population inversion gratings in laser frequency combs. *Optica* **5**, 475–478 (2018).
20. Kane, D. & Trebino, R. Characterization of arbitrary femtosecond pulses using frequency-resolved optical gating. *IEEE J. Quantum Electron.* **29**, 571–579 (1993).
21. Iaconis, C. & Walmsley, I. A. Spectral phase interferometry for direct electric-field reconstruction of ultrashort optical pulses. *Opt. Lett.* **23**, 792–794 (1998).
22. Burghoff, D. et al. Terahertz laser frequency combs. *Nat. Photon.* **8**, 462–467 (2014).
23. Burghoff, D. et al. Evaluating the coherence and time-domain profile of quantum cascade laser frequency combs. *Opt. Express* **23**, 1190–1202 (2015).
24. Khurgin, J. B., Dikmelik, Y., Hugi, A. & Faist, J. Coherent frequency combs produced by self frequency modulation in quantum cascade lasers. *Appl. Phys. Lett.* **104**, 081118 (2014).
25. Mansuripur, T. S. et al. Single-mode instability in standing-wave lasers: the quantum cascade laser as a self-pumped parametric oscillator. *Phys. Rev. A* **94**, 063807 (2016).
26. Singleton, M., Jouy, P., Beck, M. & Faist, J. Evidence of linear chirp in mid-infrared quantum cascade lasers. *Optica* **5**, 948–953 (2018).
27. Burghoff, D., Yang, Y. & Hu, Q. Computational multiheterodyne spectroscopy. *Sci. Adv.* **2**, e1601227 (2016).
28. Schwarz, B. et al. Monolithically integrated mid-infrared lab-on-a-chip using plasmonics and quantum cascade structures. *Nat. Commun.* **5**, 4085 (2014).
29. Schneider, H. & Liu, H. C. *Quantum Well Infrared Photodetectors* (Springer-Verlag, Berlin Heidelberg, 2006).

Acknowledgements

This work was supported by the Austrian Science Fund (FWF) in the framework of 'Building Solids for Function' (Project W1243), the projects 'NanoPlas' (P28914-N27) and 'NextLite' (F4909-N23). H.D. acknowledges support by the ESF under project CZ. 02.2.69/0.0/0.0/16_027/0008371. A.M.A was supported by projects COMTERA—FFG 849614 and AFOSR FA9550-17-1-0340.

Author contributions

J.H. and B.S. built up the SWIFTS set-up. J.H. carried out the experiments and wrote the manuscript, with B.S. and A.M.A. providing editorial input. H.D., A.M.A. and G.S. were responsible for MBE growth. B.S. developed the algorithm for the SWIFTS data processing and supervised this work. All authors contributed to analysing the results and commented on the paper.

Competing interests

The authors declare no competing interests.

Additional information

Supplementary information is available for this paper at https://doi.org/10.1038/s41566-018-0320-3.

Reprints and permissions information is available at www.nature.com/reprints.

Correspondence and requests for materials should be addressed to B.S.

Publisher's note: Springer Nature remains neutral with regard to jurisdictional claims in published maps and institutional affiliations.

Methods

Device. The investigated QCL is uncoated and operating at 8 µm. The laser has a relatively low group delay dispersion. The laser is mounted epi-side-up on a copper submount. The temperature of the submount is kept at 15 °C for all measurements presented using a Peltier element and a PTC5000 temperature controller. A HP 8341B synthesized sweeper is used for injection locking. The RF signal is injected close to the front end of the QCL cavity through 40 GHz two-terminal RF probes. It has to be noted that due to the large parasitic capacitance, the RF signal is strongly damped by 30–40 dB.

SWIFTS. The QWIP used to detect the optical beatnote is fabricated in a square mesa geometry with 100 µm side length. The mesa is connected to a coplanar transmission line with a short wirebond, resulting in a cutoff frequency slightly below 10 GHz. The optical beatnote detected by the QWIP is amplified and mixed down to below 50 MHz. A Zurich Instruments HF2LI lock-in amplifier and the helium–neon trigger of the FTIR were used to record the SWIFTS interferograms. To discuss this in more detail, we consider the electric field of a comb that is composed of discrete modes with amplitudes A_n and frequencies $\omega_n = \omega_0 + n\omega_r$, where n is an integer and ω_0 and ω_r are the carrier envelope offset frequency and repetition frequency of the comb. The complex sum of both quadrature interferograms can then be written as

$$(X+iY)(\tau) = \sum_n A_n A_{n-1}^{\star}\left[\cos\left(\frac{\omega_r\tau}{2}\right) + \cos\left(\omega_{n-\frac{1}{2}}\tau\right)\right] \tag{2}$$

Equation (2) differs slightly from previously published work[23,26] because our FTIR (Bruker Vertex 70v) moves both interferometer arms by $\pm\tau/2$ instead of just one arm by τ. The SWIFTS spectrum is obtained by applying a Fourier transform to the complex SWIFTS interferogram. The angled brackets denote temporal averaging of the SWIFTS signal by the lock-in amplifier. The complex phase in equation (3) is equal to the phase difference of adjacent comb lines:

$$\mathcal{F}(X+iY)(\omega) = \sum_n \langle |A_n||A_{n-1}|\, e^{i(\phi_n - \phi_{n-1})}\rangle \times\left[\delta\left(\omega-\omega_{n-\frac{1}{2}}\right) + \delta(\omega-\omega_r/2)\right] \tag{3}$$

Self-detected dual-comb spectrum. The two QCLs on the dual-comb chip are roughly 1 mm apart. The light emitted from the front facets of the dual-comb chip is collimated using an anti-reflection-coated ZnSe lens with a 1.5 inch focal length. By aligning a mirror in front of the lens, the light of one laser is reflected into the other. The dual-comb beat around 8.7 GHz is extracted directly from the laser using a RF probe and recorded with a spectrum analyser (acquisition time ≈ 0.2 s.)

Data availability

The data that support the plots within this paper and other findings of this study are available from the corresponding author upon reasonable request.